Novel Eu^{3+}-doped lead telluroborate glasses for red laser source applications

M.V. Vijaya Kumar [a], B.C. Jamalaiah [b,c,*], K. Rama Gopal [d], R.R. Reddy [d]

[a] Department of Physics, Rayalaseema University, Kurnool 518002, India
[b] Department of Physics, Sree Vidyanikethan Engineering College, Tirupati 517102, India
[c] Department of Physics, Changwon National University, Changwon 641-773, South Korea
[d] Department of Physics, Sri Krishnadevaraya University, Anantapur 515055, India

ABSTRACT

We report the absorption, luminescence and decay analysis of Eu^{3+}-doped lead telluroborate (PTBEu) glasses for different Eu^{3+} concentrations ranging from 0.1 to 2.0 mol%. Judd–Ofelt intensity parameters obtained from $^5D_0 \rightarrow {}^7F_{J=0-6}$ emission transitions of Eu^{3+} were used to calculate the radiative transition probabilities, luminescence branching ratios and radiative decay times. The luminescence spectra and decay times were measured at 464 nm excitation. The optical band gap energies are also determined. The luminescence intensity ratio, color purity and emission cross-section values support that the PTBEu20 glass is a suitable candidate for red laser source applications.

© 2011 Elsevier Inc. All rights reserved.

1. Introduction

Rare-earth ions doped glasses are important materials for bulk lasers, optical fibers, waveguide lasers, optical amplifiers and display devices [1–5]. The increasing demand for efficient lasing processes require optimized glasses as they influence the intra-configurational optical transitions of rare-earth ions quite significantly [6]. Among the trivalent rare earths, Eu^{3+} is an efficient activator for rich red color center for display devices due to its dominant $^5D_0 \rightarrow {}^7F_2$ emission transition. Owing to the non-degenerate nature of $^7F_0$ ground and $^5D_0$ excited states and relatively simple energy level system, the Eu^{3+} ions give information regarding the coordination environment. Thus, the Eu^{3+} ions have often been used as a spectroscopic probe for studying the symmetry and inhomogeneity present in different host matrices [7,8].

Since $^5D_0$ emission state of Eu^{3+} has much energy than its next lower lying level ($^7F_6$), the phonon energy of host is not a critical parameter to obtain radiative emissions from that state. However, glasses with low phonon energy are advantageous to decrease the multiphonon relaxation rates and obtain efficient radiative emission from $^5D_0$ state [7,9]. Besides, the low phonon glasses also provide an opportunity to examine unusual luminescence transitions from $^5D_{J=1,2,3}$ states of Eu^{3+}, which are not

often observed in hosts of high phonon energy [10]. Slight discrepancy in the bonding parameters such as ligand distance, ligand angle, coordination number and covalence causes a variation in the strength of ligand field and consequently in the energy levels of Eu^{3+} free ion. Thus, rare-earth luminescence spectra have been governed by coordination environment around the rare-earth ion.

In this paper, we report the absorption, luminescence and decay studies of Eu^{3+}-doped lead telluroborate (PTBEu) glasses for different Eu^{3+} concentrations (0.1, 0.5, 1.0 and 2.0 mol%). The room temperature absorption spectra were recorded in the spectral range from 500 to 2400 nm. The luminescence spectra and decay profiles were measured at 464 nm excitation. The Judd–Ofelt (J–O) theory [11,12] has been used to calculate the radiative parameters such as transition probability (A_R), radiative decay time (τ_R) and luminescence branching ratio (β_R) of an excited state. The obtained optical properties of PTBEu20 glass make it to be a promising material for red laser source applications.

2. Experimental

The PTBEu glasses used in this work were prepared with the composition in mol%: $30PbF_2 \cdot 30TeO_2 \cdot (40-x)H_3BO_3 \cdot xEu_2O_3$ ($x=0.1$, 0.5, 1.0 and 2.0) and they were referred as PTBEu01, PTBEu05, PTBEu10 and PTBEu20 glasses, respectively. Accurately weighted 10 g batches of starting materials were thoroughly

* Corresponding author at: Department of Physics, Sree Vidyanikethan Engineering College, Tirupati 517102, India. Fax: +91 877 2225211.
E-mail address: bcjamal@gmail.com (B.C. Jamalaiah).

mixed and then melted at 800–850 °C for 1 h in a silica crucible. The melts were poured in a preheated brass cast and pressed with another brass plate to get a flat disk of 2 mm thick and then annealed at 300 °C for 5 h to remove thermal strains. The obtained glasses were polished for measuring their physical and optical properties. The absorption spectrum was measured with a Perkin Elmer Lambda-950 spectrophotometer. The excitation, luminescence and decay measurements were carried out with a Jobin YVON 21 Fluorolog spectrofluorimeter with xenon flash lamp as a light source. All the measurements were carried out at room temperature only. The amorphous nature of the glasses was verified by X-ray diffraction (XRD) studies using CuKα as the radiation source. The absence of XRD peaks (not shown) indicates the amorphous nature of glasses under investigation. The refractive indices were measured using Abbes' refractometer (GE-138) with sodium vapor lamp as light source and 1-bromonapthalene as adhesive liquid. The densities were measured by the Archimedes' principle using distilled water as an immersion liquid. For all samples the refractive index and density values were found to be $\sim$1.468 and $\sim$5.385 g cm^{-3}, respectively.

3. Results and discussion

The optical absorption spectra of PTBEu glasses recorded at room temperature in the spectral range from 500 to 2400 nm exhibited six absorption bands originating from the ground ($^7F_0$) and the first excited ($^7F_1$) states, namely $^7F_0 \rightarrow ^5D_1$ ($\sim$526 nm/ $\sim$19011 cm^{-1}); $^7F_1 \rightarrow ^5D_1$ ($\sim$536 nm/$\sim$18651 cm^{-1}); $^7F_0 \rightarrow ^5D_0$ ($\sim$574 nm/$\sim$17422 cm^{-1}); $^7F_1 \rightarrow ^5D_0$ ($\sim$586 nm/$\sim$17065 cm^{-1}); $^7F_0 \rightarrow ^7F_6$ ($\sim$2070 nm/$\sim$4831 cm^{-1}) and $^7F_1 \rightarrow ^7F_6$ ($\sim$2230 nm/ $\sim$4484 cm^{-1}). The intensities of these bands increase with the increase of Eu^{3+} dopant concentration. The absorption band positions and their relative intensities are agreed well with our earlier reports in different hosts [13–15]. For reference, the absorption spectrum of PTBEu20 glass is shown in Fig. 1. The inset figure illustrates the variation of absorbance of $^7F_0 \rightarrow ^7F_6$ transition in PTBEu glasses. The partial energy level diagram shown in Fig. 2 describes the absorption transitions of Eu^{3+} noticed in PTBEu glasses under investigation.

It is well known fact that the absorption spectrum of Eu^{3+} contains absorption transitions not only from the ground state ($^7F_0$) but also from the first excited state ($^7F_1$) due to closely spaced
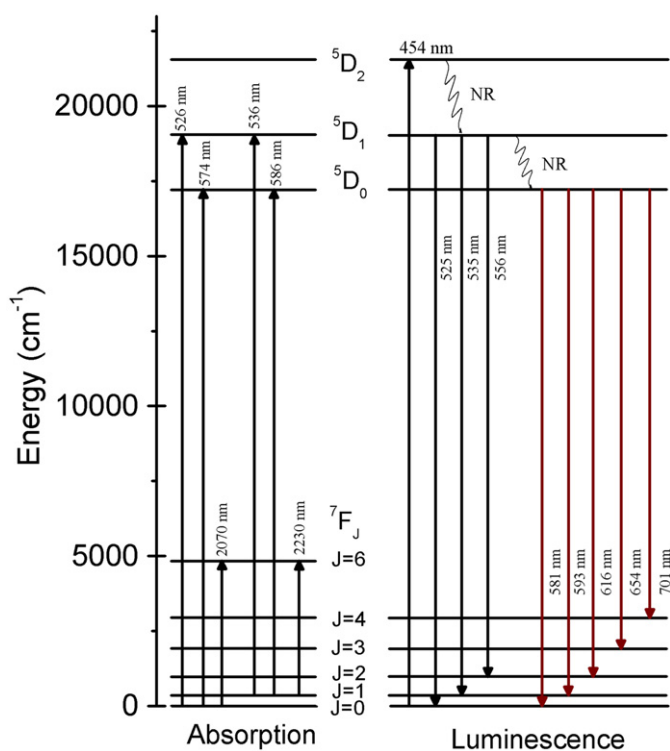
Fig. 2. Partial energy level diagram showing the possible absorption and luminescence transitions of Eu^{3+} ions in PTBEu glasses.

$^7F_0$ and $^7F_1$ states. The close examination of absorption band positions of ($^7F_0$, $^7F_1$) $\rightarrow ^5D_1$, $^5D_0$ and $^7F_6$ transitions indicate that the energy gap between the ground ($^7F_0$) and the first excited ($^7F_1$) states is about $\sim$350 cm^{-1}. Theoretically it is of the order of KT ($\sim$203 cm^{-1}), where K is the Boltzmann's constant and T is the absolute temperature [16]. At room temperature (293 K) the fractional thermal population of $^7F_1$ level cannot be neglected because $\sim$65% Eu^{3+} ions populate $^7F_0$ ground state, $\sim$30% Eu^{3+} ions populate the first excited state $^7F_1$ and the rest of $\sim$5% Eu^{3+} ions can populate other higher excited states. For any excited state, the fractional thermal population can be calculated using a well known expression [17]. The procedure based on fractional thermal population was described in detail in our previous work [13–15]. The values of fractional thermal population for ground, first and second excited states are found to be 0.66, 0.31 and 0.02, respectively, and very close to LTTEu20 [13], Eu:RLTB [14] and LBTAF [15] glasses.

The optical band gap (E_g) is an important parameter used to describe a solid-state laser material. In amorphous materials, the relation between the absorption coefficient [$\alpha(v)$] and phonon energy (hv) of incident radiation can be written as [18]: $(\alpha hv) = B(hv - E_g)^n$, where B is a constant and E_g is the optical band gap energy. The index 'n' can have values 2, 3, 1/2 and 1/3 for indirect allowed, indirect forbidden, direct allowed and direct forbidden transitions, respectively. In various glass systems, the above equation depicts a straight line for indirect allowed transition (n=1/2). The values of E_g can be determined from linear region of the Tauc's curves [hv vs. $(\alpha hv)^{1/2}$] shown in Fig. 3, which were extrapolated to meet the hv axis at $(\alpha hv)^{1/2}$=0. The E_g values are found to be $\sim$2.60 eV with an accuracy of $\pm$0.01 eV for PTBEu glasses. From Fig. 3 one can observe a negligible deviation in the values of E_g. This deviation might be due to the experimental errors only.

The excitation spectra of luminescence at 616 nm were recorded in the spectral region 350–500 nm. Since all the glasses show similar results, the excitation spectrum of PTBEu20 glass is shown in Fig. 4 as reference. The excitation spectrum revealed
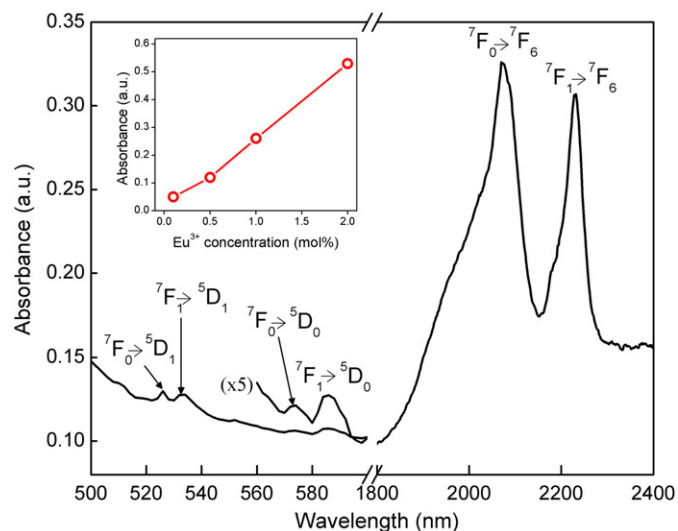
Fig. 1. Absorption spectrum of the PTBEu20 glass. Inset is the variation of absorbance of $^7F_0 \rightarrow ^7F_6$ transition with Eu^{3+} concentration.
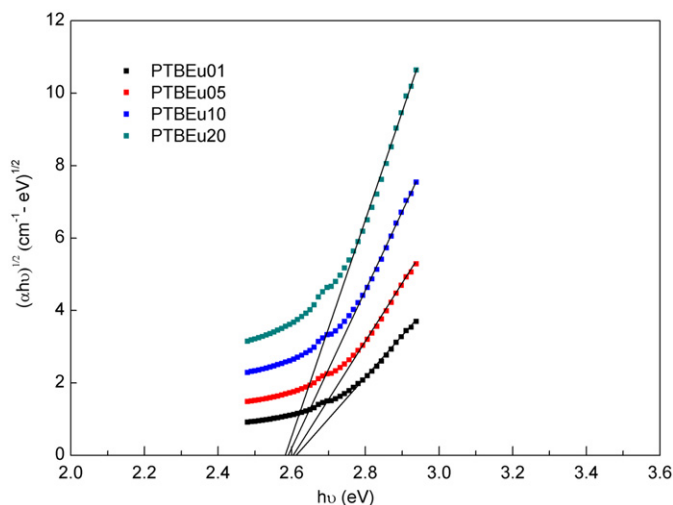
Fig. 3. $h\upsilon$ vs. $(\alpha h\upsilon)^{1/2}$ plots for PTBEu glasses.
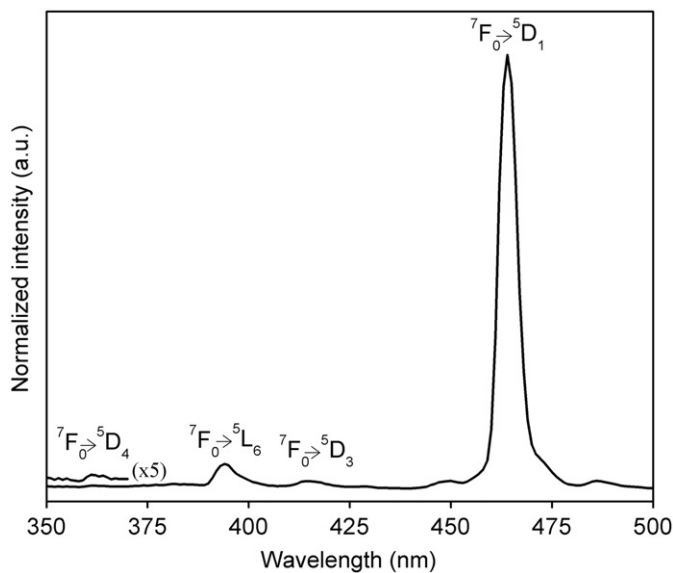
Fig. 4. Excitation spectrum ($\lambda_{em}=616$ nm) of the PTBEu20 glass.

Fig. 5. Luminescence spectrum ($\lambda_{ex}=464$ nm) of the PTBEu20 glass. Inset shows the variation of intensity of $^5D_0\rightarrow{}^7F_2$ (616 nm) transition with Eu^{3+} concentration.

four bands such as $^7F_0\rightarrow{}^5D_4$ (360 nm), $^7F_0\rightarrow{}^5L_6$ (394 nm), $^7F_0\rightarrow{}^5D_3$ (414 nm) and $^7F_0\rightarrow{}^5D_1$ (464 nm). Among these, the $^7F_0\rightarrow{}^5D_1$ (464 nm) transition is found to be more prominent and it was used to record the luminescence spectra of PTBEu glasses in the 500–750 nm spectral range. These spectra displayed a total of eight transitions: $^5D_1\rightarrow{}^7F_0$ (525 nm); $^5D_1\rightarrow{}^7F_1$ (535 nm); $^5D_1\rightarrow{}^7F_2$ (556 nm); $^5D_0\rightarrow{}^7F_0$ (580 nm); $^5D_0\rightarrow{}^7F_1$ (593 nm); $^5D_0\rightarrow{}^7F_2$ (616 nm); $^5D_0\rightarrow{}^7F_3$ (654 nm) and $^5D_0\rightarrow{}^7F_4$ (700 nm). The emission spectra of PTBEu glasses are normalized with reference to the intensity of the $^5D_0\rightarrow{}^7F_2$ (616 nm) transition of PTBEu20 glass. Fig. 5 illustrates a normalized emission spectrum of PTBEu20 glass. The possible radiative transitions of Eu^{3+} in PTBEu glasses are presented in the partial energy level diagram described in Fig. 2. Obviously, the luminescence intensity of observed transitions increases with increase of Eu^{3+} concentration. For example, the variation of luminescence intensity of a prominent emission transition centered at 616 nm ($^5D_0\rightarrow{}^7F_2$) with Eu^{3+} ion concentration is depicted as inset in Fig. 5.

The shielding effects of $4f$ electrons by $5s$ and $5p$ electrons in outer shells of Eu^{3+} ion result narrow emission bands. In the studied glasses, the effective bandwidth ($\Delta\lambda_P$) of the characteristic
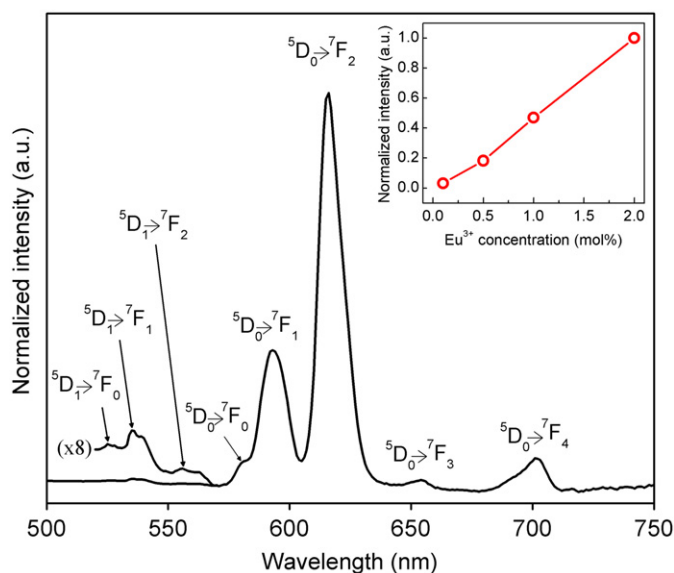
emission band of Eu^{3+} due to $^5D_0\rightarrow{}^7F_2$ transition is found to be decreased slightly with the increase of Eu^{3+} concentration (see Table 2). This variation might be due to within the experimental errors. It is well known fact that the emission intensity of $\Sigma^5D_0\rightarrow{}^7F_J$ represents the total intensity of Eu^{3+}-doped glasses. Since the emissions due to $^5D_{3,2,1}\rightarrow{}^7F_J$ transitions are several orders smaller than that of $^5D_0\rightarrow{}^7F_J$ transitions, the emissions from these three excited states are suppressed [19]. When the Eu^{3+} ions are excited to any level above the $^5D_0$, there is a fast non-radiative multiphonon relaxation to this level. The excited Eu^{3+} ions at $^5D_0$ level relaxes radiatively through $^5D_0\rightarrow{}^7F_J$ transitions, since the large energy difference of $\sim$12600 cm^{-1} between $^5D_0$ and $^7F_6$ levels prevents the possibility of multi-phonon relaxation (see Fig. 2). The $^5D_0\rightarrow{}^7F_2$ transition is identified as a hypersensitive electric dipole transition ($\Delta J=2$) in Eu^{3+} and it has been strongly influenced by the coordination environment. The $^5D_0\rightarrow{}^7F_1$ transition ($\Delta J=1$) has been identified as a magnetic dipole transition. The luminescence intensity ratio (R) between electric ($^5D_0\rightarrow{}^7F_2$) and magnetic ($^5D_0\rightarrow{}^7F_1$) dipole transitions provide valuable information about the red color ($^5D_0\rightarrow{}^7F_2$) richness in comparison with orange ($^5D_0\rightarrow{}^7F_1$) color in developing red laser sources. This intensity ratio is a measure of degree of Eu^{3+}–O^{2-} covalence and symmetry around the Eu^{3+} ions [20,21]. Generally, the value of R is proportional to the Eu^{3+}–O^{2-} covalence i.e., the higher the R value, the lower the symmetry around Eu^{3+} ion is. On the other hand, the local symmetry and/or covalence changes around the Eu^{3+} ion at higher concentrations. The values of R (see Table 1) increased with increase of Eu^{3+} concentration as shown in Fig. 6b. The Commission Internationale de I'Eclairage (CIE) coordinates and color purity values of these glasses are calculated following Ref. [22] and documented in Table 1. When the concentration of Eu^{3+} is raised from 0.1 to 2.0 mol% the CIE coordinates shifted towards red color and the magnitude of color purity changes from 8% to 74%. As can be seen from Fig. 7 and color purity values, one can suggest that the PTBEu20 glass emits rich red color than other glasses under this study.

Since the $^5D_0\rightarrow{}^7F_{J=0-6}$ transitions of Eu^{3+} depend on coordination environment of host material, these transitions have been used to calculate the J–O intensity parameters ($\Omega_{\lambda=2,4,6}$) [23]. Upon 464 nm excitation, the PTBEu glasses exhibited $^5D_0\rightarrow{}^7F_{J=0-4}$

Table 1
Values of J–O intensity parameters ($\Omega_\lambda \times 10^{-20}$ cm^2), intensity ratio (R), CIE coordinates and color purity for PTBEU glasses.

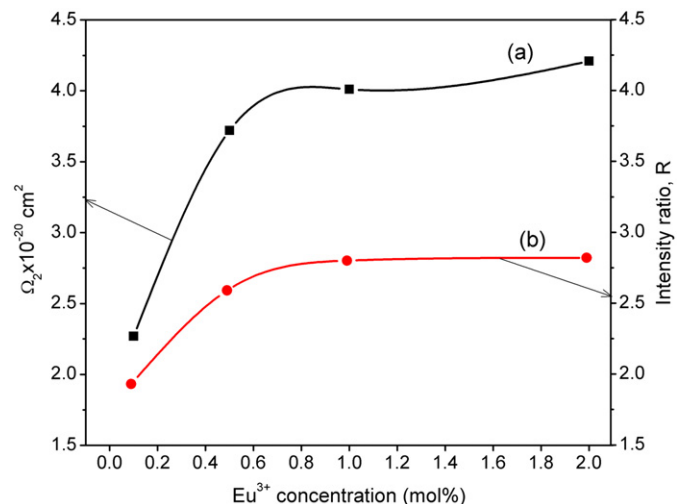| Glass	J–O parameters			R	CIE coordinates		Color purity
	Ω_2	Ω_4	Ω_6		x-	y-	
PTBEu01	2.27	5.22	~0	1.93	0.344	0.294	8
PTBEu05	3.72	1.78	~0	2.59	0.474	0.335	49
PTBEu10	4.01	1.21	~0	2.80	0.506	0.321	60
PTBEu20	4.21	0.80	~0	2.82	0.547	0.329	74

Fig. 6. Variation of Ω_2 intensity parameter (a) and luminescence intensity ratio (b) with Eu^{3+} concentration in PTBEu glasses.
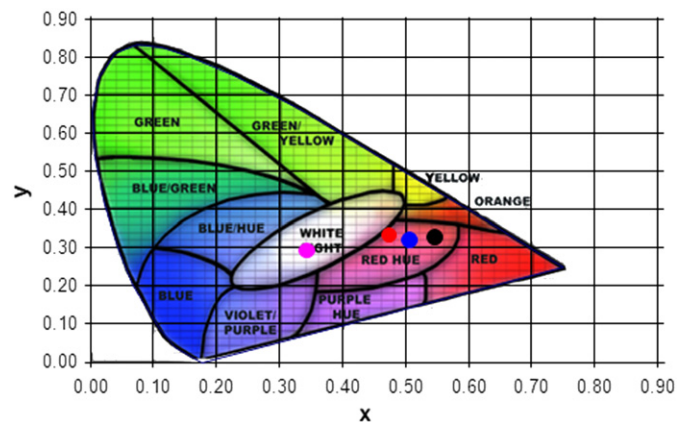

Fig. 7. Location of CIE coordinates of PTBEu glasses (Pink-PTBEu01; Red-PTBEu05; Blue-PTBEu10 and Black-PTBEu20). (For interpretation of the references to color in this figure legend, the reader is referred to the web version of this article.)

transitions in addition to $^5D_1 \rightarrow {}^7F_{0,1,2}$ transitions in the spectral region $500-750$ nm. Using the intensities of $^5D_0 \rightarrow {}^7F_{J=0-4}$ transitions, Ω_2 and Ω_4 intensity parameters are determined (see Table 1). However, Ω_6 parameter is not obtained due to the absence of $^5D_0 \rightarrow {}^7F_6$ transition. Reasonably very weak transitions centered at ~ 750 nm ($^5D_0 \rightarrow {}^7F_5$) and ~ 810 nm ($^5D_0 \rightarrow {}^7F_6$) are not identified due to the limitations of JOBIN YVON Fluorolog-3 spectrofluorimeter. Thus, the Ω_6 parameter is taken as zero in determining radiative properties such as spontaneous probability (A_R), radiative decay time (τ_R) and luminescence branching ratio (β_R). The magnitude of Ω_2 parameter depends on Eu^{3+}–O^{2-} covalence and also explains the symmetry of coordination environment around Eu^{3+} ion [5]. However, the Ω_4 and Ω_6 parameters

have been related to bulk properties of host matrix. The Ω_2 parameter increase monotonically with increase of Eu^{3+} ion concentration (see Fig. 6a) and consequently decrease the symmetry around Eu^{3+} ion and then increase Eu^{3+}–O^{2-} covalence. The Ω_2 obtained for PTBEu20 glass is found higher than those reported in the literature [7,13,24].

The evaluated set of J–O intensity parameters obtained from $^5D_0 \rightarrow {}^7F_J$ transitions can be used to determine several radiative properties of PTBEu glasses by well known expressions [13–15]. Some of the radiative properties for a prominent emission band centered at 616 nm ($^5D_0 \rightarrow {}^7F_2$) are displayed in Table 2. The transition probabilities (A_R), experimental (β_{exp}) and predicted (β_R) branching ratios and stimulated emission cross-sections (σ_e) are found to be increased in the order: PTBEu01 → PTBEu05 → PTBEu10 → PTBEu20. The luminescence branching ratio characterizes the lasing power of an emission transition and a potential laser transition should have a branching ratio of ≥ 0.50. The stimulated emission cross-section together with effective bandwidth and radiative decay time are used to calculate the gain bandwidth ($\sigma_e \times \Delta\lambda_P$) and optical gain ($\sigma_e \times \tau_R$) parameters, which are critical to predict the amplification of a medium in which the rare-earth ions are situated. In the present study, the values of ($\sigma_e \times \Delta\lambda_P$) and ($\sigma_e \times \tau_R$) are found to be increased with increase of Eu^{3+} ion concentration. The calculated radiative parameters of PTBEu20 glass indicate its suitability as a rich red laser source than other glasses under investigation and also other reported Eu^{3+} doped different hosts [25–27].

The decay profiles of the $^5D_0$ emission state of Eu^{3+} ions in PTBEu glasses were recorded under excitation at 464 nm and emission at 616 nm. All the decay profiles are well fitted to a single exponential function: $I_t = I_o e^{-t/\tau}$, where I_t is the actual luminescence intensity, I_o is the luminescence intensity at the start of the decay process, t is the time and τ is the decay time. The average decay time changes from 2.10 to 2.22 ms when Eu^{3+} concentration is changed from 0.1 to 2.0 mol%. The radiative decay time can be calculated using the J–O theory [11,12]. Table 3 presents the experimental (τ_{ave}) and radiative (τ_R) decay times of PTBEu glasses. As the decay times are nearly equal to one another, the decay curve of $^5D_0$ emission state in PTBEu20 glass is shown in Fig. 8 (as reference). The decay times support the

Table 2
Radiative parameters of $^5D_0 \rightarrow {}^7F_2$ (616 nm) level of Eu^{3+} ion in PTBEu glasses.

Radiative parameter	PTBEu01	PTBEu05	PTBEu10	PTBEu20
Effective bandwidth, $\Delta\lambda_P$ (nm)	15.04	13.00	12.61	12.35
Transition probability, A_R (s^{-1})	65.35	107.22	115.49	121.19
Luminescence branching ratio, β_R	0.35	0.60	0.65	0.68
Experimental branching ratio, β_{exp}	0.25	0.59	0.61	0.65
Emission cross-section, σ_e ($\times 10^{-22}$ cm^2)	3.85	7.31	8.12	8.70
Gain bandwidth, $\sigma_e \times \Delta\lambda_P$ ($\times 10^{-28}$ cm^3)	5.79	9.50	10.24	10.74
Optical gain, $\sigma_e \times \tau_R$ ($\times 10^{-24}$ cm^2 s)	2.07	4.11	4.56	4.89

Table 3
Radiative (τ_R), experimental (τ_{ave}) decay time, non-radiative rate (W_{NR}) and quantum efficiency (η) of $^5D_0$ emission level of Eu^{3+} in PTBEu glasses.

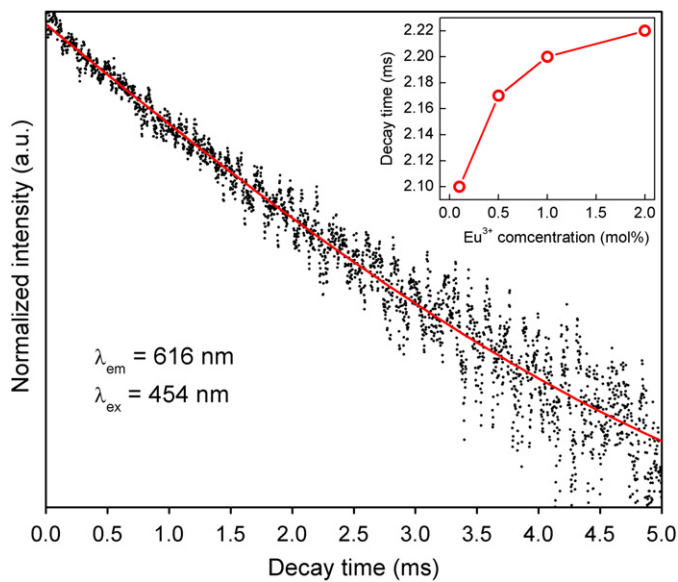| Glass host	τ_{ave} (in ms)	τ_R (in ms)	W_{NR} (in s^{-1})	η (in %)
PTBEu01	2.10	5.38	290	39
PTBEu05	2.14	5.62	281	39
PTBEu10	2.20	5.62	277	39
PTBEu20	2.22	5.62	272	40

Fig. 8. Logarithmic plot of the luminescence decay of $^5D_0$ state of Eu^{3+} in PTBEu20 glass. Inset presents the Eu^{3+} concentration vs. decay time in PTBEu glasses.

increase in luminescence intensity of $^5D_0 \rightarrow {}^7F_2$ transition in PTBEu glasses. It is obvious that the decay time increases with increase of Eu^{3+} ion concentration due to the decrease in symmetry around Eu^{3+}. The inset of Fig. 8 describes the variation of decay time as a function of Eu^{3+} ion concentration in PTBEu glasses. The deviation of τ_{ave} values from τ_R is due to non-radiative decay rates (W_{NR}) from $^5D_0$ state of Eu^{3+} and are listed in Table 3. The quantum efficiency, $\eta = \tau_{ave}/\tau_R$, is a measure of the number of photons emitted per excited ion. For all the glasses the quantum efficiency is found to be $\sim$40% (see Table 3).

4. Conclusions

Different concentrations of Eu^{3+} ions doped PTBEu glasses were prepared by melt quenching method and characterized through absorption, luminescence and decay measurements. The J–O intensity parameters were calculated using the intensities of $^5D_0 \rightarrow {}^7F_{J=0-6}$ transitions of Eu^{3+} ion. The red color richness of the $^5D_0 \rightarrow {}^7F_2$ (616 nm) transition has been obtained using the

intensity ratio $[R=({}^5D_0 \rightarrow {}^7F_2)/({}^5D_0 \rightarrow {}^7F_1)]$ values. The decay profiles are well fitted to a single exponential function and the decay time of the $^5D_0$ emission state is increased with increase of Eu^{3+} concentration. The effective bandwidth and the stimulated emission cross-section values for $^5D_0 \rightarrow {}^7F_2$ transition in PTBEu20 glass are 12.35 nm and 8.70×10^{-22} cm^2, respectively. The gain bandwidth and optical gain parameters are 10.74×10^{-28} cm^3 and 4.89×10^{-24} cm^2 s, respectively. Based on the observed optical properties we suggest that the PTBEu20 glass is a suitable solid state material for red laser (616 nm) source applications.

References

[1] V. Scarnera, B. Richards, A. Jha, G. Jose, C. Stacey, Opt. Mater. 33 (2010) 159–163.
[2] L. Huang, A. Jha, S. Shen, W.Jin Chung, Opt. Commun. 239 (2004) 403–408.
[3] X.J. Li, E.Y.B. Pun, Y.Y. Zhang, H. Lin, Physica B 403 (2008) 3509–3513.
[4] G. Lakshminarayana, Hucheng Yang, Jianrong Qiu, J. Solid State Chem. 182 (2009) 669–676.
[5] T. Som, B. Karmakar, Phys. Condens. Matter 22 (2010) 035603 (11pp.).
[6] C.H. Kam, S. Buddhudu, Physica B 344 (2004) 182–189.
[7] D. Zhao, X. Qiao, X. Fan, M. Wang, Physica B 395 (2007) 10–15.
[8] R. Balda, J. Fernandez, J.L. Adam, M.A. Arriandiaga, Phys. Rev. B 54 (1996) 12076–12086.
[9] W.A. Pisarski, J Pisarska, G. Dominiak-Dzik, W. Ryba-Romanowski, J. Phys.: Condens. 16 (2004) 6171–6184Matter 16 (2004) 6171–6184.
[10] A. Kumar, D.K. Rai, S.B. Rai, Spectrochim. Acta A 58 (2002) 2115–2125.
[11] B.R. Judd, Phys. Rev. 127 (1962) 750–755.
[12] G.S. Ofelt, J. Chem. Phys. 37 (1962) 511–514.
[13] A. Mohan Babu, B.C. Jamalaiah, T. Suhasini, T. Srinivasa Rao, L. Rama Moorthy, Solid State Sci. 13 (2011) 574–578.
[14] S.A. Saleem, B.C. Jamalaiah, A. Mohan Babu, K. Pavani, L. Rama Moorthy, J. Rare Earths 28 (2010) 189–193.
[15] B.C. Jamalaiah, J. Suresh Kumar, A. Mohan Babu, L. Rama Moorthy, J. Alloys Compd. 478 (2009) 63–67.
[16] M. Dejneka, E. Snitzer, R.E. Riman, J. Lumin. 65 (1995) 227–245.
[17] R. Van Deun, K. Binnemans, C. Görller-Walrand, J.L. Adam, J. Phys. Condens. Matter 10 (1998) 7231–7241.
[18] N.F. Mott, E.A. Davis, Electronic Processes in Non-Crystalline Materials, second ed., Oxford University Press, Oxford, 1979.
[19] D.R. Tallant, C.H. Seager, R.L. Simpson, J. Appl. Phys. 91 (7) (2002) 4053 (12pp.).
[20] A. Patra, E. Sominska, S. Ramesh, Y. Koltypin, Z. Zhong, H. Minti, R. Reisfeld, A. Gedanken, J. Phys. Chem. B 103 (1999) 3361–3365.
[21] G. Ehrhart, M. Bouazaoui, B. Capoen, V. Ferreiro, R. Mahiou, O. Robbe, S. Turrell, Opt. Mater. 29 (2007) 1723–1730.
[22] E.Fred Schubert, Light-Emitting Diodes, second ed., Cambridge University Press, New York, 2006.
[23] H. Ebendorff-Heide Priem, D. Ehrt, J. Non-Cryst. Solids 208 (1996) 205–216.
[24] B.J. Chen, E.Y.B. Pun, H. Lin, J. Alloys Compd. 479 (2009) 352–356.
[25] W.A. Pisarski, Phys. Status Solidi 242 (2005) 2910–2918.
[26] X.J. Lu, E.Y.B. Pun, Y.Y. Zhang, H. Lin, Physica B 403 (2008) 3508–3513.
[27] K. Marimuthu, S. Surendra Babu, G. Muralidharan, S. Arumugam, C.K. Jayasankar, Phys. Status Solidi 206 (2009) 137–139.